Reflective Coating Optimization for Interferometric Detectors of Gravitational Waves

Maria Principe

University of Sannio at Benevento, INFN, LVC and KAGRA

*principe@unisannio.it

Abstract: Brownian fluctuations in the highly reflective test-mass coatings are the dominant noise source, in a frequency band from a few tens to a few hundreds Hz, for Earth-bound detectors of Gravitational Waves. Minimizing such noise is mandatory to increase the visibility distance of these instruments, and eventually reach their quantum-limited sensitivity. Several strategies exist to achieve this goal. Layer thickness and material properties optimization have been proposed and effectively implemented, and are reviewed in this paper, together with other, so far less well developed, options. The former is the simplest option, yielding a sensible noise reduction with limited technological challenges; the latter is more technologically demanding, but is needed for future (cryogenic) detectors.

OCIS codes: (310.1620, 310.4165, 310.6628)

References and links

1. J.M. Weisberg and J.H. Taylor, "The Relativistic Binary Pulsar B1913+16: Thirty Years of Observations and Analysis" ASP Conf.Ser. **328** (2005) 25.
2. A. Einstein, "Über Gravitationswellen,"Sitzungberichte der Königlich Preussischen Akad. der Wissenschaften Berlin, 154, (1918).
3. B.F. Schutz, "Gravitational Wave Astronomy," Class. Quantum Grav. **16**, A131 (1997).
4. P. Saulson, "*Fundamentals of Interferometric Gravitational Wave Detectors*," World Scientific, Singapore (1994).
5. B. C. Barish and R. Weiss, "LIGO and the Detection of Gravitational Waves," Physics Today **52**, 44 (1999).
6. H. Luck and the GEO600 team, "The GEO600 Project," Class. Quantum Grav. **14**, 1471 (1997).
7. B. Caron, A. Dominjon, C. Drezen, R. Flaminio, X. Grave, F. Marion, L. Massonnet, C. Mehmel, R. Morand, B. Mours, V. Sannibale, M. Yvert, D. Babusci, S. Bellucci, S. Candusso, G. Giordano, G. Matone, J.-M. Mackowski, L. Pinard, F. Barone, E. Calloni, L. Di Fiore, M. Flagiello, F. Garufi, A. Grado, M. Longo, M. Lops, S. Marano, L. Milano, S. Solimeno, V. Brisson, F. Cavalier, M. Davier, P. Hello, P. Heusse, P. Mann, Y. Acker, M. Barsuglia, B. Bhawal, F. Bondu, A. Brillet, H. Heitmann, J.-M. Innocent, L. Latrach, C.N. Man, M. Pham-Tu, E. Tournier, M. Taubmann, J.-Y. Vinet, C. Boccara, P. Gleyzes, V. Loriette, J.-P. Roger, G. Cagnoli, L. Gammaitoni, J. Kovalik, F. Marchesoni, M. Punturo, M. Beccaria, M. Bernardini, E. Bougleux, S. Braccini, C. Bradaschia, G. Cella, A. Ciampa, E. Cuoco, G. Curci, R. Del Fabbro, R. DeSalvo, A. Di Virgilio, D. Enard, I. Ferrante, F. Fidecaro, A. Giassi, A. Giazotto, L. Holloway, P. La Penna, G. Losurdo, S. Mancini, M. Mazzoni, F. Palla, H.-B. Pan, D. Passuello, P. Pelfer, R. Poggiani, R. Stanga, A. Vicer, Z. Zhang, V. Ferrari, E. Majorana, P. Puppo, P. Rapagnani and F. Ricci, "The Virgo Interferometer," Class. Quantum Grav. **14**, 1461 (1997).
8. K. Kawabe and the TAMA collaboration,"Status of TAMA Project," Class. Quantum Grav. **14**, 1477 (1997).
9. D. G. Blair, "The First Stage of the Laser Interferometer Gravitational Wave Observatory in Australia," Gen. Rel. Grav. **32**, 371 (2000).
10. C.S. Unnikrishnan, "IndIGO and LIGO-India: Scope and Plans for Gravitational Wave Research and Precision Metrology in India," Int. J. Mod. Phys. D, **22**, 1341010 (2013)
11. K. Kuroda, "Status of LCGT," Class. Quantum Grav. **27**, 084004 (2010).

12. M. Punturo, M. Abernathy, F. Acernese, B. Allen, N. Andersson, K. Arun, F. Barone, B. Barr, M. Barsuglia, M. Beker, N. Beveridge, S. Birindelli, S. Bose, L. Bosi, S. Braccini, C. Bradaschia, T. Bulik, E. Calloni, G. Cella, E. Chassande Mottin, S. Chelkowski, A. Chincarini, J. Clark, E. Coccia, C. Colacino, J. Colas, A. Cumming, L. Cunningham, E. Cuoco, S. Danilishin, K. Danzmann, G. De Luca, R. De Salvo, T. Dent, R. De Rosa, L. Di Fiore, A. Di Virgilio, M. Doets, V. Fafone, P. Falferi, R. Flaminio, J. Franc, F. Frasconi, A. Freise, P. Fulda, J. Gair, G. Gemme, A. Gennai, A. Giazotto, K. Glampedakis, M. Granata, H. Grote, G. Guidi, G. Hammond, M. Hannam, J. Harms, D. Heinert, M. Hendry, I. Heng, E. Hennes, S. Hild, J. Hough, S. Husa, S. Huttner, G. Jones, F. Khalili, K. Kokeyama, K. Kokkotas, B. Krishnan, M. Lorenzini, H. Lck, E. Majorana, I. Mandel, V. Mandic, I. Martin, C. Michel, Y. Minenkov, N. Morgado, S. Mosca, B. Mours, H. MllerEbhardt, P. Murray, R. Nawrodt, J. Nelson, R. Oshaughnessy, C. D. Ott, C. Palomba, A. Paoli, G. Parguez, A. Pasqualetti, R. Passaquieti, D. Passuello, L. Pinard, R. Poggiani, P. Popolizio, M. Prato, P. Puppo, D. Rabeling, P. Rapagnani, J. Read, T. Regimbau, H. Rehbein, S. Reid, L. Rezzolla, F. Ricci, F. Richard, A. Rocchi, S. Rowan, A. Rdiger, B. Sassolas, B. Sathyaprakash, R. Schnabel, C. Schwarz, P. Seidel, A. Sintes, K. Somiya, F. Speirits, K. Strain, S. Strigin, P. Sutton, S. Tarabrin, A. Thring, J. van den Brand, C. van Leewen, M. van Vegge, C. van den Broeck, A. Vecchio, J. Veitch, F. Vetrano, A. Vicere, S. Vyatchanin, B. Willke, G. Woan, P. Wolfango and K. Yamamoto, "The Einstein Telescope: a Third-Generation Gravitational Wave Observatory," Class. Quantum Grav. **27**, 194002 (2010).
13. http://www.lisa.nasa.gov; www; https://www.elisascience.org/;
14. S. Kawamura, M. Ando, N. Seto, S. Sato, T. Nakamura, K. Tsubono, N. Kanda, T. Tanaka, J. Yokoyama, I. Funaki, K. Numata, K. Ioka, T. Takashima, K. Agatsuma, T. Akutsu, K.-S. Aoyanagi, K. Arai, A. Araya, H. Asada, Y. Aso, D. Chen, T. Chiba, T. Ebisuzaki, Y. Ejiri, M. Enoki, Y. Eriguchi, M.-K. Fujimoto, R. Fujita, M. Fukushima, T. Futamase, T. Harada, T. Hashimoto, K. Hayama, W. Hikida, Y. Himemoto, H. Hirabayashi, T. Hiramatsu, F.-L. Hong, H. Horisawa, M. Hosokawa, K. Ichiki, T.Ikegami, K. T. Inoue, K. Ishidoshiro, H. Ishihara, T. Ishikawa, H. Ishizaki, H. Ito, Y. Itoh, K. Izumi, I. Kawano, N. Kawashima, F. Kawazoe, N. Kishimoto, K. Kiuchi, S. Kobayashi, K. Kohri, H. Koizumi, Y. Kojima, K. Kokeyama, W. Kokuyama, K. Kotake, Y. Kozai, H. Kunimori, H. Kuninaka, K. Kuroda, S. Kuroyanagi, K.-I. Maeda, H. Matsuhara, N. Matsumoto, Y. Michimura, O. Miyakawa, U. Miyamoto, S. Miyoki, M. Y. Morimoto, T. Morisawa, S. Moriwaki, S. Mukohyama, M. Musha, S. Nagano, I. Naito, K. Nakamura, H. Nakano, K. Nakao, S. Nakasuka, Y. Nakayama, K. Nakazawa, E. Nishida, K. Nishiyama, A. Nishizawa, Y. Niwa, T. Noumi, Y. Obuchi, M. Ohashi, N. Ohishi,, M. Ohkawa, K. Okada, N. Okada, K. Oohara, N. Sago, M. Saijo, R. Saito, M. Sakagami, S.-I. Sakai, S. Sakata, M. Sasaki, T. Sato, M. Shibata, H.Shinkai, A. Shoda, K. Somiya, H. Sotani, N. Sugiyama, Y. Suwa, R. Suzuki, H. Tagoshi, F. Takahashi, K. Takahashi, K. Takahashi, R. Takahashi, R. Takahashi, T. Takahashi, H. Takahashi, T. Akiteru, T. Takano, N. Tanaka, K. Taniguchi, A. Taruya, H. Tashiro, Y. Torii, M. Toyoshima, S. Tsujikawa, Y. Tsunesada, A. Ueda, K.-I. Ueda, M. Utashima, Y. Wakabayashi, K. Yagi, H. Yamakawa, K. Yamamoto, T. Yamazaki, C.-M. Yoo, S. Yoshida, T. Yoshino and K.-X. Sun, "The Japanese Space Gravitational Wave Antenna: DECIGO", Class. Quantum Grav. **28**, 094011 (2011).
15. W.T. Ni, "ASTROD and ASTROD I - Overview and Progress,". Int. J. Mod. Phys. **D 17**, 921 (2008).
16. P.W. McNamara, "The LISA Pathfinder Mission," Int. J. Mod. Phys. **D22** 1341001 (2013).
17. M. Ando and the DECIGO Working Group, "DECIgo Pathfinder," Int. J. Mod. Phys. **D22**, 1341002 (2013) .
18. G. M. Harry, H. Armandula, E. Black, D. R. M. Crooks, G. Cagnoli, J. Hough, P. Murray, S. Reid, S. Rowan, P. Sneddon, M. M. Fejer, R. Route, and S. D. Penn, "Thermal Noise from Optical Coatings in Gravitational Wave Detectors," Applied Opt. **45**, 1569 (2006).
19. The LIGO Scientific Collaboration, "A Gravitational Wave Observatory Operating beyond the Quantum Shot-Noise Limit," Nature Phys. **7**, 92 (2011).
20. G.M. Harry, T. P. Bodiya, and R. DeSalvo, Eds., "Optical Coatings and Thermal Noise in Precision Measurements," Cambridge Univ. Press, Cambridge UK (2012).
21. T. Hong, H. Yang, E. K. Gustafson, R. X. Adhikari, and Y. Chen, "Brownian Thermal Noise in Multilayer Coated Mirrors," Phys Rev D **87**, 082001 (2013).
22. A.E. Villar, E. D. Black, R. DeSalvo, K. G. Libbrecht, C. Michel, N. Morgado, L. Pinard, I. M. Pinto, V. Pierro, V. Galdi, M. Principe, and I. Taurasi, "Measurement of Thermal Noise in Multilayer Coatings with Optimized Layer Thickness," Phys. Rev. D **81**, 122001 (2010).
23. M. Principe, I. M. Pinto, V. Pierro, R. DeSalvo, I. Taurasi A.E. Villar, E. D. Black, R. DeSalvo, K. G. Libbrecht, C. Michel, N. Morgado and L. Pinard, "Material Loss Angles from Direct Measurements of Broadband Thermal Noise," Phys. Rev. D (2013) in print.
24. D.R.M. Crooks, G. Cagnoli, M. M. Fejer, G. Harry, J. Hough, B. T. Khuri-Yakub, S. Penn, R. Route, S. Rowan, P. H. Sneddon, I. O. Wygant, and G. G. Yaralioglu, "Experimental Measurements of Mechanical Dissipation Associated with Dielectric Coatings Formed Using SiO_2, Ta_2O_5 and Al_2O_3," Class. Quantum Grav. **23** 4953 (2006).
25. J. Agresti, G. Castaldi, R. DeSalvo, V. Galdi, V. Pierro, and I. M. Pinto, "Optimized Multilayer Dielectric Mirror Coatings for Gravitational Wave Interferometers," SPIE Proceedings Vol. 6286, "*Advances in Thin-Film Coatings for Optical Applications,*" M.J. Ellison, Ed., 628608 (2006).
26. E. Black, A. Villar, K. Barbary, A. Bushmaker, J. Heefner, S. Kawamura, F. Kawazoe, L. Matone, S. Meidt, S. R. Rao, K. Schulz, M. Zhang, K. G. Libbrecht, "Direct Obsrvation of Broadband Coating Thermal Noise in a

Suspended Interferometer," Phys. Lett. A **328**, 1 (2004).
27. V. Pierro, I. M. Pinto, and M. Principe, "Coating Optimization Status," LIGO Document G0900205 (2009).
28. M. Principe, I. M. Pinto, V. Pierro, and R. DeSalvo, "Minimum Brownian Noise Dichroic Dielectric Mirror Coatings for AdLIGO," LIGO Document T080337, (2008).
29. A. Villar, "Measurement of Brownian Noise in Ti-doped Tantala Coatings," LIGO Document G0900887.
30. G.M. Harry, M.R. Abernathy, A.E. Becerra-Toledo, H. Armandula, E. Black, K. Dooley, M. Eichenfield, C. Nwabugwu, A. Villar, D.R.M. Crooks, G. Cagnoli, J. Hough, C.R. How, I. MacLaren, P. Murray, S. Reid, S. Rowan, P.H. Sneddon, M.M. Fejer, R. Route, S.D. Penn, P. Ganau, J. Mackowski, C. Michel, L. Pinard and A. Remillieu., "Titania-Doped Tantala/Silica Coatings for Gravitational-Wave Detection," Class. Quantum Grav. **24**, 40 (2006).
31. R.P. Netterferld and M. Gross, "Investigation of Ion-Beam-Sputtered Silica-Titania Mixtures for Use in Gravitational Wave Interferometer Optics," Proc. OSA/OIC Conference, Tucson AZ, USA (2007), paper ThD2.
32. K.S. Gilroy and W.A. Phillips, "An Asymmetric Double-Well Potential Model for Structural relaxation Processes in Amorphous Materials," Phil. Mag. **B43**, 745 (1981).
33. J. Trinastic, R.Hamdan, Y. Wu, L. Zhang, H. Cheng, "Combined Interatomic Potential for Pure and Doped Tantala, Titania, Hafnia, and Silica," LIGO Document P1300028 (2013).
34. R. Bassiri, M.R. Abernathy, R.L. Byer, K. Craig, E.K. Gustafson, M.M. Fejer, M. Hart, J. Hough, N. Kim, B. Lantz, A.C. Lin, I. MacLaren, A.S. Markosyan, I.W. Martin, S.C. McGuire, A. Mehta, P. Murray, S.D. Penn, R.K. Route, S. Rowan and J.F. Stebbins, "Atomic Structure Investigations of Heat-Treated and Doped Tantala Coatings," LIGO Document G1400271.
35. R. Flaminio, J. Franc, C. Michel, N. Morgado, L. Pinard and B. Sassolas, "A Study of Coating Mechanical and Optical Losses in view of Reducing Mirror Thermal Noise in Gravitational Wave Detectors," Class. Quantum Grav. **27**, 084030 (2010).
36. I.M. Pinto, M. Principe and R. DeSalvo, "Effective Medium Theory for Modeling Dielectric Mixture Properties, " LIGO Document G1100372 (2011).
37. O. Stenzel, S. Wilbrandt, M. Schürmann, N. Kaiser, H. Ehlers, M. Mende, D. Ristau, S. Bruns, M. Verghl, M. Stolze, M. Held, H. Niederwald, T. Koch, W. Riggers, P. Burdack, G. Mark, R. Schfer, S. Mewes, M. Bischoff, M. Arntzen, F. Eisenkrmer, M. Lappschies, S. Jakobs, S. Koch, B. Baumgarten, and A. Tnnermann , "Mixed Oxide Coatings for Optics," Appl. Opt., **50**, C69 (2011).
38. D. A. G. Brüggeman, "Berechnung Verschiedener Physikalischer Konstanten von Heterogenen Substanzen - I. Dielektrizittskonstanten und Leitfhigkeiten der Mischkrper aus Isotropen Substanzen," Ann. Phys. **24** (1935) 637.
39. S. Barta, "Effective Young's Modulus and Poisson's Ratio for the Particulate Composite ," J. Appl. Phys. **75**, 3258 (1994).
40. I.M. Pinto, M. Principe and R. DeSalvo, "Subwavelength layered Titania-Silica for Advanced Interferometer Coatings," LIGO Document G1100586 (2011).
41. M. Born and E. Wolf, *Principles of Optics*, Cambridge University Press, 1980.
42. A. Reuss,"Berchung der Fiessgrenze von Mischkristallen auf Grund der Plastiziatsbedingung fur Einkristalle," Z. Angew. Math. Mech. **09**, 49 (1929).
43. W. Voigt, "Uber die Beziehung Zwischen Den Beiden Elastiziatskonstanten Isotroper Korper," Wied. Ann. **38**, 537 (1889).
44. W.-H. Wang and S.Chao, "Annealing Effect on Ion Beam Sputtered Titanium Dioxide Films," Opt. Lett., **23**, 1417 (1998).
45. S.V. Ushakov, A. Navrotsky, Y. Yang, S. Stemmer, K. Kukli, M. Ritala, M.A. Leskel, P. Fejes, A. Demkov, C. Wang, B.-Y. Nguyen, D. Triyoso and P. Tobin, "Crystallization in Hafnia and Zirconia Based Systems," Phys. Stat. Sol. **B 241**, 2268 (2004).
46. S. Penn, J. Luo, R. Kasturi, and J. Podkaminer, "Recent Measurements of Coating and Substrate Mechanical Loss for aLIGO, LIGO document G10009321 (2010).
47. H. Sankur and W. Gunning, "Crystallization and Diffusion in Composite TiO_2/SiO_2 Thin Films," J. Appl. Phys. **66**, 4747 (1989).
48. M. Liu, G. He, L.Q. Zhu, Q. Fang, G.H. Li and L.D. Zhang, "Microstructure and Interfacial Properties of HfO_2/Al_2O_3 Nanolaminate Films," Appl. Surf. Sci., **252**, 6206 (2006).
49. H.-W. Pan, S.-J. Wang, L.-C. Kuo, S.Chao, M. Principe, I.M. Pinto and R. DeSalvo "Thickness Dependent Crystallization on Thermal Annealing for Titania-Silica nm-Layered Composites Deposited by Ion Beam Sputtering Method," Optics Express **22**, 29847 (2014).
50. I. Pinto, M. Principe, R. DeSalvo, S. Chao, H.-W. Pan and L.C. Kuo, "nm-Layered Amorphous Glassy Oxide Composites for 3rd Generation Interferometric GW Detectors," LIGO Document G14001358 (2014).
51. M. Fernndez-Perea, M.-A. Descalle, R. Soufli, K. P. Ziock, J. Alameda, S. L. Baker, T. J. McCarville, V. Honkim´aki, E. Ziegler, A. C. Jakobsen, F. E. Christensen, and M. J. Pivovaroff, Physics of Reflective Optics for the Soft Gamma-Ray Photon Energy Range, Phys. Rev. Lett. 111, 027404 (2013)
52. R. Soufli, Breakthroughs in Photonics 2013: X-Ray Optics, IEEE Photonics J., **6**, 0700606 (2014)
53. I.W. Martin, H Armandula, C. Comtet, M.M. Fejer, A. Gretarsson, G. Harry, J- Hough, J-M. M. Mackowski,

I. MacLaren, C. Michel, J-L. Montorio, N. Morgado, R. Nawrodt, S. Penn, S. Reid, A. Remillieux, R. Route, S. Rowan, C. Schwarz, P. Seidel, W. Vodel and A. Zimmer, "Measurements of a Low-Temperature Mechanical Dissipation Peak in a Single Layer of Ta_2O_5 Doped with TiO_2," Class. Quantum Grav., **25**, 055005 (2008).
54. I.W. Martin, R. Bassiri, R. Nawrodt, M.M. Fejer, A. Gretarsson, E. Gustafson, G. Harry, J. Hough, I. MacLaren, S. Penn, S. Reid, R. Route, S. Rowan, C. Schwarz, P. Seidel, J. Scott and A.L. Woodcraft, "Effect of Heat Treatment on Mechanical Dissipation in Ta2O5 Coatings," Class. Quantum Grav. **. 27**, 225020 (2010).
55. M. R. Abernathy, S. Reid, E. Chalkley, R. Bassiri, I.W. Martin, K. Evans, M.M. Fejer, A. Gretarsson, G.M. Harry, J. Hough, I. MacLaren, A. Markosyan, P. Murray, R. Nawrodt, S. Penn, R. Route, S. Rowan and P. Seidel, "Cryogenic Mechanical Loss Measurements of Heat-Treated Hafnium Dioxide," Class. Quantum Grav. **28**, 195017 (2011).
56. W. W. Scott and R.K. MacCrone, "Apparatus for Mechanical Loss Measurements in Low Loss Materials at Audio Frequencies and Low Temperatures," Rev. Sci. Instr. **39** 821 (1968).
57. S. Pond, "Stress Reduction in Ion Beam Sputtered Mixed Oxide Films," Appl. Optics, **28**, 2800 (1989).
58. S. Chao, W.-H. Wang and C.-C. Lee, "Low-Loss Dielectric Mirror with Ion-Beam-Sputtered $TiO_2 - SiO_2$ Mixed Films," Optics Lett. **40**, 2177 (2001).
59. P. Murray, "Coating Mechanical Loss Investigations," LIGO Document G-1400275
60. S. Chao, work in progress (2014).
61. M.G. Tarallo, J. Miller, J. Agresti, E. D'Ambrosio, R. DeSalvo, D. Forest, B. Lagrange, J.M. Mackowsky, Ch. Michel, J.L. Montorio, N. Morgado, L. Pinard, A. Remilleux, B. Simoni, and P. Willems, "Generation of a Flat-Top Laser Beam for Gravitational Wave Detectors by Means of a Nonspherical Fabry - Perot Resonator," Applied Opt. **46**, 6648 (2007).
62. V. Galdi, G. Castaldi, V. Pierro, I. M. Pinto, J. Agresti, E. D'Ambrosio, R. DeSalvo, "Analytic Structure of a Family of Hyperboloidal Beams of Potential Interest for Advanced LIGO," Phis. Rev. **D73**, 127101 (2006).
63. M. Bondarescu, O. Kogan and Y. Chen, "Optimal Light Beams and Mirror Shapes for Future LIGO Interferometers," Phys. Rev **D78**, 08002 (2008).
64. V. Pierro, V. Galdi, G. Castaldi, I. M. Pinto, J. Agresti, R. DeSalvo, "Perspectives on Beam-Shaping Optimization for Thermal-Noise Reduction in Advanced Gravitational-Wave Interferometric Detectors: Bounds, Profiles, and Critical Parameters," Phys. Rev. **D76**, 122003 (2007).
65. M. Granata, C. Buy, R. Ward, and M. Barsuglia, "Higher-Order Laguerre-Gauss Mode Generation and Interferometry for Gravitational Wave Detectors," Phys. Rev. Lett. **105**, 231102 (2010).
66. B. Sorazu, P.J. Fulda, B.W. Barr, A.S. Bell, C. Bond, L. Carbone, A. Freise, S. Hild, S.H. Huttner, J. Macarthur and K. A. Strain, "Experimental Test of Higher-Order Laguerre-Gauss Modes in the 10 m Glasgow Prototype Interferometer," Class. Quantum Grav., **30** 035004 (2013).
67. A.G. Gurkovski, D. Heinert, S. Hild, R. Nawrodt, K. Somiya, S.P. Vyatchanin and H. Wittel, "Reducing Thermal Noise in Future Gravitational Wave Detectors by Employing Khalili Etalons," Phys. Lett. **A375**, 4147 (2011).
68. S. Gossler, J. Cumpston, K. McKenzie, C.M. Mow-Lowry, M.B. Gray, and D.E. McClelland, "Coating-Free Mirrors for High Precision Interferometric Experiments," Phys. Rev. **A76**, 053810 (2007).
69. A. Bunkowski, O. Burmeister, D. Friedrich, K. Danzmann and R. Schnabel, "High Reflectivity Grating Waveguide Coatings for 1064 nm", Class. Quantum Grav. **23**, 7297 (2006).
70. G. D. Cole, W. Zhang, M.J. Martin, J. Ye and M. Aspelmeyer, "Tenfold Reduction of Brownian Noise in High-Reflectivity Optical Coatings," Nature Photonics **7**, 644 (2013).
71. A. Lin, R. Bassiri, K. Craig, A. Cumming, M. Fejer, J. Harris, K. Haughian, J. Hough, A. Markosyan, I. Martin, P. Murray, R. Route, and S. Rowan., "Prospects and Progress in Crystalline Coatings: AlGaP," LIGO Document G1300580 (2013).

1. Introduction

Gravitational waves (GWs), for which only indirect evidence exists to date [1], are predicted by Einstein relativistic theory of gravitation [2]. Their detection will open a new and unique window on the Universe [3]. GWs are ripples in the spacetime fabric produced by massive cosmic objects in accelerated motion, and can be detected using very long baseline optical interferometers [4]. Several interferometric detectors have been constructed, are being upgraded, or have been planned world-wide, including LIGO [5], GEO [6], VIRGO [7], TAMA [8], ACIGA [9], INDIGO [10], KAGRA (formerly LCGT) [11], and ET [12], in an unprecedented multinational effort. Space-borne interferometric detectors have been also envisaged [13], [14], [15], and are under development [16], [17]. The sensitivity of Earth-bound detectors is limited by noises of different origin (e.g., seismic, thermal and quantum, see Figure 1). The noise power spectral density of these instruments is minimum in a frequency band between a few tens and a few hundreds Hz, where several cosmic sources of gravitational waves are deemed to exist [3].

In this frequency band the dominant noise source are the Brownian fluctuations in the highly reflective coatings of the test masses making up the end-mirrors of the interferometer arms [18]. Minimizing coating Brownian noise is a must to reach (and eventually beat [19]) the sensitivity quantum limit. A reduction of the noise floor level by a factor p entails a $p^{-3/2}$ boost of the instrument visibility volume [4].
In this paper several proposed approaches to coating Brownian noise minimization are reviewed, with special emphasis on ideas contributed by the Author's research group, namely as regards coating geometry and materials optimization strategies.

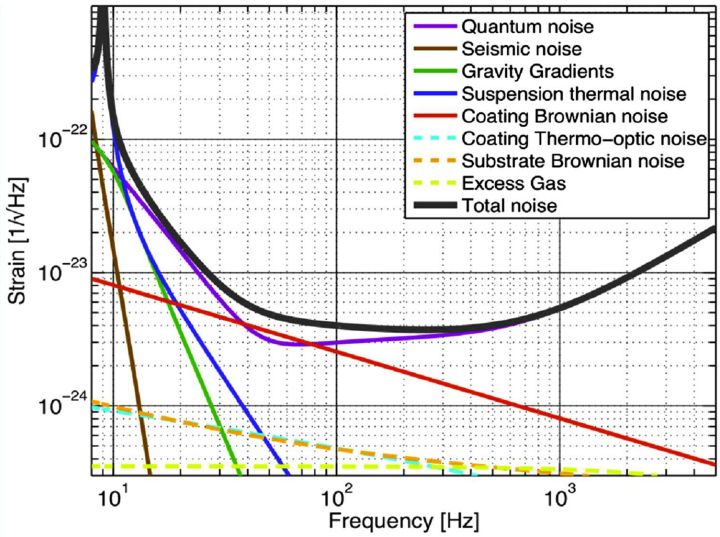

Fig. 1. Noise power spectral density budget of the advanced LIGO detector in strain (gravitational wave amplitude) units.

2. Coating Thermal Noise

Using the fluctuation-dissipation theorem, the Brownian noise power spectral density in the interferometer test-mass mirror coatings can be cast in the form [18]

$$S_B(f) = \frac{2k_B T}{\pi^{3/2} f} \frac{(1-\sigma_s^2)}{w Y_s} \phi_c, \tag{1}$$

where k_B is Boltzmann's constant, T the absolute temperature, w the half-width of the (Gaussian) laser beam, σ_s and Y_s are the Poisson's ratio and Young's elastic modulus of the substrate, and ϕ_c is the effective mechanical loss angle of the coating. To reduce S_B one thus could: i) cool the mirrors (i.e., decrease T); ii) expand the illuminated area (i.e., increase w); iii) reduce the coating loss angle ϕ_c. Here I shall focus on the third option; the other two will be shortly discussed in Section 5 .
Coatings are currently made of alternating layers of two dielectric materials (amorphous glassy oxides) with different refractive indexes. In the limit where the materials' Poisson's ratios are vanishingly small, we have a simple formula for the coating loss angle [20]:

$$\phi_c = b_L Z_L + b_H Z_H, \tag{2}$$

where $Z_{L,H}$ are the total optical thicknesses (i.e., thicknesses in units of the local wavelength) of the lower (L) and higher (H) index material, given by the product of the number of layers,

$N_{L,H}$, and the optical thicknesses of the individual layers, $z_{L,H}$, and

$$b_{L,H} = \frac{\lambda_0}{\sqrt{\pi} w} \frac{\phi_{L,H}}{n_{L,H}} \left(\frac{Y_{L,H}}{Y_s} + \frac{Y_s}{Y_{L,H}} \right). \tag{3}$$

represent the *specific* material loss angles (i.e., the loss angles per unit optical thickness), being $n_{L,H}$ and $\phi_{L,H}$ the refractive index and mechanical loss angle of the lower and higher index material, respectively, and λ_0 the operating wavelength. A different, and putatively more accurate coating noise formula has been recently proposed, where the material viscoelastic properties are described in terms of the (complex) shear and bulk moduli [21]. This approach reproduces eqs. (2)-(3) if the bulk and shear loss-angles are equal. While this is rarely the case, eqs. (2)-(3) agree fairly well with available measurements of coating and material loss angles [22], [23] and will be adopted hereinafter. The quarter-wavelength (QWL, or Bragg) coating design, where the thickness of the individual layers is $z_{L,H} = 1/4$, yields the minimum number of layers to achieve a prescribed transmittance [20], and is the usual choice for all applications where coating noise is not an issue.

Material downselection led to the choice of SiO_2 (Silica) and Ta_2O_5 (Tantala) as the best available materials for the highly reflective (henceforth HR) coatings for GW detectors in a pool of many (pure) amorphous glassy oxides, including SiO_2, HfO_2, ZrO_2, TiO_2, Al_2O_3, Sc_2O_3, Y_2O_3, Ta_2O_5 and Nb_2O_5 [24], yielding the best tradeoff among high dielectric contrast (large ratio n_H/n_L), low optical absorption (small extinction coefficients κ), and low thermal noise (small specific loss angles $b_{L,H}$).

In view of eq. (2) two possible strategies are envisaged to minimize the effective coating loss angle. Having chosen the low (SiO_2) and high (Ta_2O_5) index materials, $n_{L,H}$ and $b_{L,H}$ are fixed, and the only free parameters in the coating design are the layers' thicknesses $z_{L,H}$. The second strategy consists in seeking better materials (natural or artificially engineered), featuring a better tradeoff between a large refraction index and a small mechanical loss angle.

3. Coating Thickness Optimization

Genetic optimization, where *no* a-priori assumption is made about the total number of layers and the thicknesses of the individual layers, shows that (except for the coating top and bottom layers), the optimal coating consisted of a stack of *equal* doublets, with optical thicknesses $z_{L,H}$ such that $z_L + z_H = 1/2$, and $z_H < 1/4 < z_L$ [25]. This is not surprising, since for the chosen materials (Silica-Tantala) $b_H \approx 10 b_L$.

The number of free design parameters can be accordingly reduced to four: the total number N_d of doublets, a quantity $\xi \in (0, 1/4)$, such that $z_{L,H} = 1/4 \pm \xi$, and the optical thicknesses of the top and bottom layers, z_T and z_B.

Coating optimization is most easily implemented *sequentally* through the following steps [20]: i) start from the quarter wavelength design with (power) transmittance τ_0 closest to the design value, and consisting of $N_d = N_0$ doublets; ii) add one doublet, and adjust the layers thicknesses (by varying the single parameter ξ) to make the coating transmittance equal to τ_0; iii) calculate the loss angle ϕ_c, and repeat step ii) until ϕ_c reaches a minimum. This procedure results into a *shallow* minimum, as shown in Figure 2, suggesting that the optimal design is robust against possible inaccuraccies in the assumed values of $b_{L,H}$, and unavoidable coating deposition tolerances [20]. The final steps consists in: iv) adjusting the thickness z_B of the bottom (H)-layer to minimize noise, and v) adjusting the thickness z_T of the top (L)-layer to bring back the transmittance to τ_0. The above coating optimization procedure was used to produce a batch of mirrors suited for the Caltech *Thermal Noise Interferometer* (TNI), an instrument designed for the *direct* measurement of coating thermal noise [26], shown in Figure 3. The optimized prototypes designed at the University of Sannio were manufactured by LMA (Laboratoire Ma-

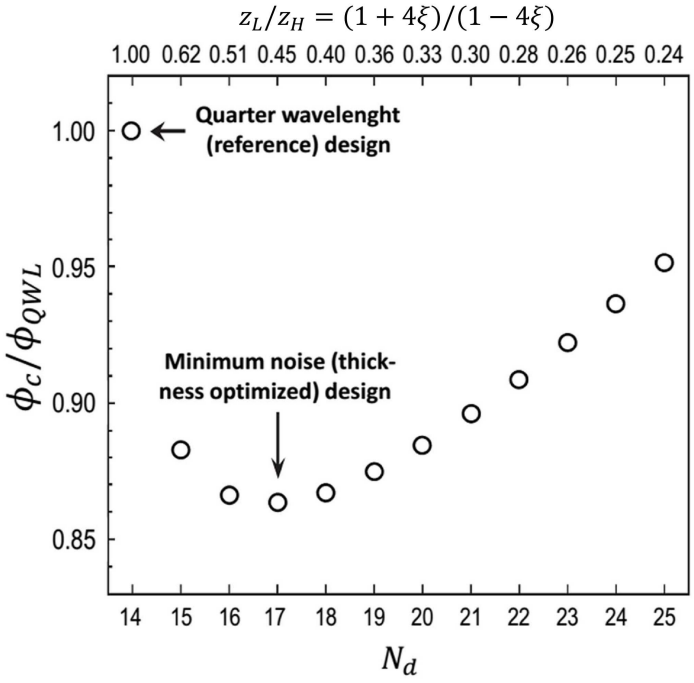

Fig. 2. Loss angle (normalized to that of the reference quarter-wavelengh design) of Silica/Tantala coatings with identical transmittance (here $287 ppm$) but different number N_d of doublets, and different layer thicknesses $z_{L,H}$. The quarter wavelength and minimum noise (optimized thickness) designs are indicated.

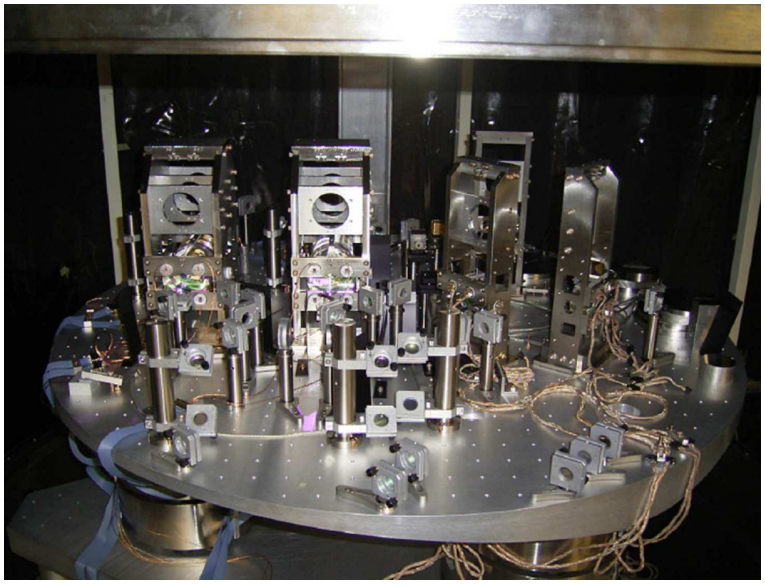

Fig. 3. The Caltech Thermal Noise Interferometer with its vacuum dome lifted (courtesy A. Villar).

teriaux Avancés of CNRS-In2P3, Lyon, FR).
The optimized coating thermal noise was measured to high accuracy, and compared to that of standard quarter-wavelength coatings having the *same* transmittance ($\tau = 287$ ppm @1064 nm). The optimized and reference (quarter-wavelength) coating designs are sketched in Figure 4. The measurement setup, and the data analysis procedure are described in detail in [22]. The meas-

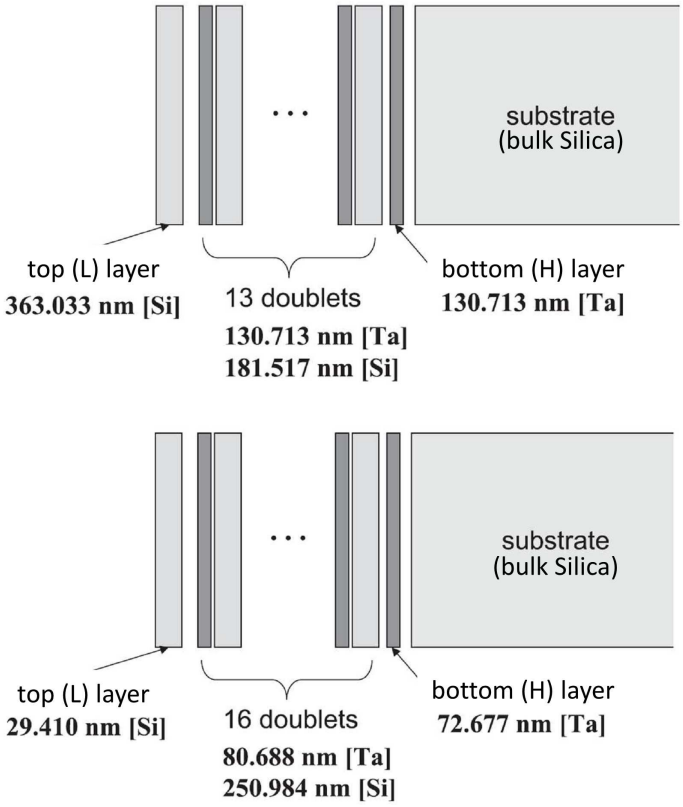

Fig. 4. Structure of the reference (quarter-wavelength, top) and thickness optimized (bottom) TNI coating prototypes.

ured loss angle of the optimized coatings was lower by a factor $p = 0.82 \pm 0.04$ compared to that of the quarter wavelength coatings. This value is in excellent agreement, within the estimated uncertainty range of the measurements and the nominal accuracy of the material parameters, with our modeling predictions [22], confirming the validity and effectiveness of the thickness optimization strategy described above.

3.1. Optimized Dichroic Coatings

Advanced (2nd generation) interferometers will use the 2nd harmonic of the laser beam for alignment purposes. The test mass coatings must be accordingly *dichroic*, i.e. besides being highly reflective at the fundamental wavelength λ_0 (with typical transmittances of a few ppm), they should provide some reflectance also at $\lambda_1 = \lambda_0/2$ (with typical power reflectance around 0.9). In view of this, the above optimization procedure was generalized to the case where the coating transmittance is constrained at two different wavelengths.

The originally proposed (reference) dichroic coating design for AdLIGO consists of a stack of N_1 doublets grown on top of the mirror substrate, with geometrical thicknesses $z_{L,H}^{(1)}$ such that

$$n_H(\lambda_1)z_H^{(1)} = \frac{\lambda_1}{4},\ n_L(\lambda_1)z_L^{(1)} = \frac{3\lambda_1}{4}, \tag{4}$$

topped by a second stack of N_0 doublets with geometrical thicknesses $z_{L,H}^{(0)}$ such that

$$n_H(\lambda_0)z_H^{(0)} = n_L(\lambda_0)z_L^{(0)} = \frac{\lambda_0}{4}. \tag{5}$$

Neglecting chromatic dispersion in the materials, i.e. assuming $n_{L,H}(\lambda_0) = n_{L,H}(\lambda_1) = n_{L,H}$, eq. (5) entails

$$n_H z_H^{(0)} = n_L z_L^{(0)} = \frac{\lambda_1}{2}, \tag{6}$$

hence, at $\lambda = \lambda_1$ the top stack is transparent, and the bottom stack, which is effectively quarter-wavelength, is designed to provide the prescribed reflectance, by choosing an appropriate N_1. From eq. (4) it follows that

$$n_H z_H^{(1)} = \frac{\lambda_0}{8},\ n_L z_L^{(1)} = \frac{3\lambda_0}{8}, \tag{7}$$

hence, at $\lambda = \lambda_0$, the bottom stack contributes part of the required reflectance, and the top stack, which is quarter-wavelength, is designed to boost the reflectance to the prescribed level, by choosing an appropriate N_0 [27].

In order to shed light on the structure of minimal noise dichroic coatings, without making any a-priori assumption about the number and thickness of the individual layers, nor neglecting chromatic dispersion in the materials, we resorted again to genetic optimization to seek coating configurations which minimize the coating Brownian noise under a *dichroic* transmittance constraint [27].

Genetically optimized coatings were found to consist of a stack of equal doublets (except for the coating top and bottom layers) with thicknesses $z_{L,H}$ such that $z_H < 1/4 < z_L$ at $\lambda = \lambda_0$, similar to the single-wavelenght case. At variance with this latter, however, in the dichroic case $z_L + z_H \neq 1/2$.

The number of free design parameters is accordingly reduced to *five*: the total number N_d of doublets, two quantities $\xi_{L,H} \in (0, 1/4)$, such that $z_L = 1/4 + \xi_L$ and $z_H = 1/4 - \xi_H$ at $\lambda = \lambda_0$, and the optical thicknesses z_T and z_B of the top and bottom layers.

The optimization strategy in the dichroic case reduces to the following [28]: i) find by trial-and-error the *minimum* value of N_d (the number of doublets) for which the region $\Sigma(N_d)$ in the (ξ_L, ξ_H) plane where the dichroic transmittance requirements are statisfied is *not* empty; ii) identify the point $\{\xi_L^*, \xi_H^*\} \in \Sigma(N_d)$ where the coating loss angle is minimum, let it be $\phi_c^*(N_d)$; iii) add one doublet and repeat step ii) until $\phi_c^*(N_d)$ reaches a global minimum.

The thickness z_B and z_T of the bottom (H) and top (L) layer can be adjusted for further noise reduction, similar to the single wavelength case, or to enforce additional requirements (e.g., to minimize the electric field intensity on the coating face, to prevent dust contamination). The shape of the $\Sigma(N_d)$ region in the (ξ_L, ξ_H) plane is sketched in Figure 5 for $N_d = 19$, with the contour curves corresponding to the constraints on transmittance @1064nm and reflectance @532nm. Following the above procedure we designed optimized dichroic coatings for advanced LIGO (AdLIGO), using Silica and Titania-doped Tantala as the low and high index materials. The optimized design features a smoother spectral response compared to the original design, as shown in Figure 6. A prototye dichroic coating consisting a down-scaled version of the AdLIGO end-test mass coating designed for a reflectance of $\sim$ 278ppm @1064nm), was

manufactured at LMA. The prototype had 12 doublets, with $\xi_L = 0.018$ and $\xi_H = 0.036$; the top and bottom layers had $\xi_L = 0.022$ and $\xi_H = 0.029$, respectively, [23], yielding a minimum of the electric field at the coating face.. TNI measurements at Caltech showed a a reduction of

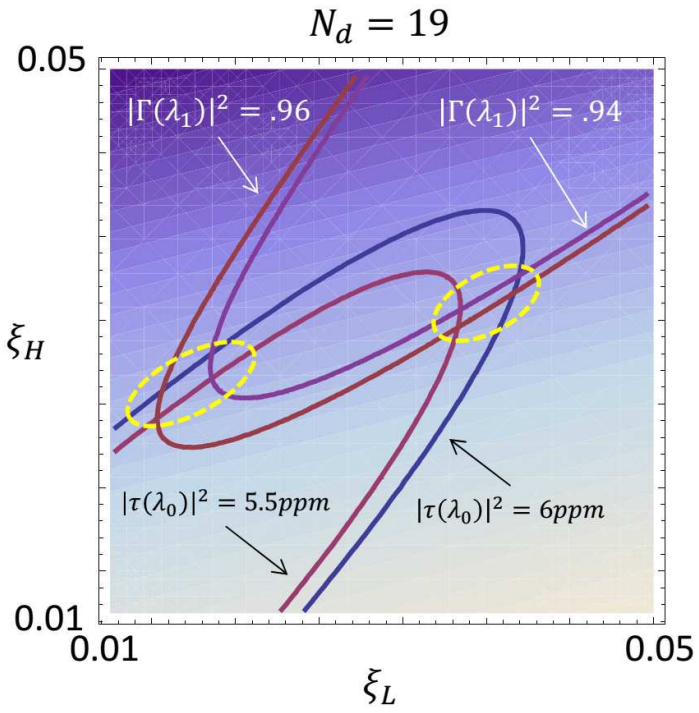

Fig. 5. Constant transmittance/reflectance loci in the (ξ_L, ξ_H) plane for a 19-doublets Silica/Tantala coating. The $\Sigma(N_d)$ region for dichroic response constraints of the interval type (AdLIGO) consists of two disjoint subsets (highlighted by the dashed yellow loops), which collapse into two distinct points in the case of equality constraints. Darker/lighter blue shades indicate higher/lower Brownian noise levels.

the loss angle by a factor ~ 0.82 compared to the single-wavelength optimized prototype using plain Tantala for the high index material, in agreement with our modeling predictions [29].

4. Materials' Properties Optimization

Coating Brownian noise can be also reduced by acting on the relevant material properties, affecting the specific loss angles $b_{L,H}$ and the refraction indexes $n_{L,H}$. Indeed, as seen from eq.s 2, 3 ,smaller $b_{L,H}$ values, and larger values of the contrast ratio n_H/n_L that reduce the number of layers needed to achieve a prescribed reflectance, imply lower thermal noise.
The most successful attempts in this direction led to the development of $TiO_2 :: Ta_2O_5$ (Titania-Tantala) [30] and $TiO_2 :: SiO_2$ (Titania-Silica) [31] mixtures.
Mechanical losses in amorphous materials are associated with thermally activated local transitions between the minima of asymmetric bistable potentials, associated to quasi-degenerate bond states [20], and can be computed from knowledge of (the distributions of) their relevant parameters [32]. Chemical doping and/or post-deposition annealing affect these parameters in various ways. Modeling efforts to deduce the above parameters from first principles are ongoing [33], [34]. Present knowledge, however, is *not* sufficient for engineering amorphous glassy

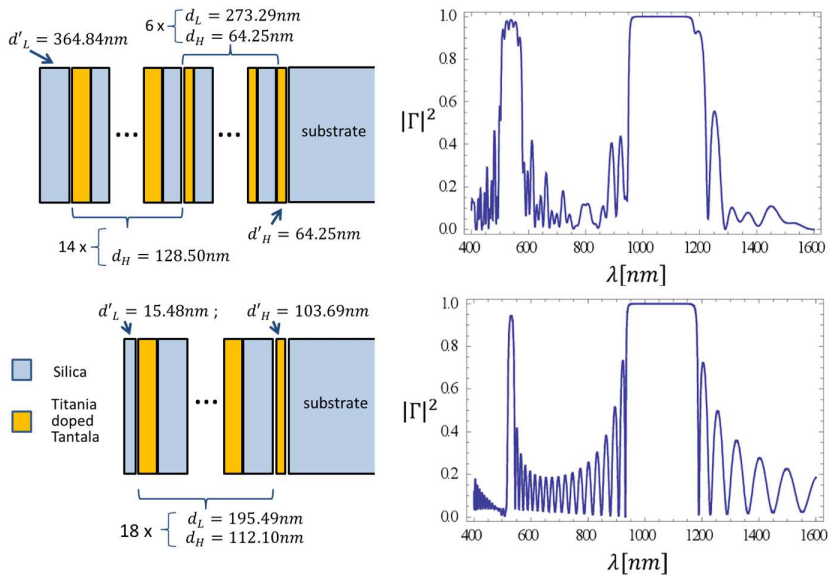

Fig. 6. Sketch (left column) and spectral response (right column) of reference (top) and thickness optimized (bottom) dichroic coating for the LIGO end-test-mass (ETM) mirror. .

oxide mixtures with prescribed properties, nor even for improving existing ones, and the quest for better coating materials is still based on extensive trial-and-error (see e.g. [35]).
An extremely simple approach to estimate the optical and mechanical properties of composite coating materials, based on effective medium theory (EMT) was proposed in [36]. Effective medium theory has been already proven to be a viable approach for optimizing the optical properties of coating glassy mixtures [37]. The refractive index $n_{mix} = \sqrt{\varepsilon_{mix}}$ of amorphous mixtures is well modeled by Bruggemann formula [38], yielding

$$\eta_2 \frac{\varepsilon_2 - \varepsilon_{mix}}{\alpha\varepsilon_2 + (1-\alpha)\varepsilon_{mix}} + (1-\eta_2)\frac{\varepsilon_1 - \varepsilon_{mix}}{\alpha\varepsilon_1 + (1-\alpha)\varepsilon_{mix}} = 0, \tag{8}$$

where η is the volume fraction, the suffixes $1,2$ and *mix* denote the constituents and the composite materials, respectively, and α is a shape factor depending on the morphology of the inclusions (we shall assume $\alpha = 3$, appropriate for spherical inclusions).
Bruggeman theory can be reformulated to compute the visco-elastic properties of amorphous composites [38]. The effective Young's modulus Y and the Poisson's ratio σ, can, e.g., be obtained, following the physically neat formulation by Barta [39], by solving the following system

$$\begin{cases} (1-\eta_2)\dfrac{X_{mix} - X_1}{2X_{mix} + (X_1/y_1)(\sigma_1+1)} + \\ \quad +\eta_2 \dfrac{X_{mix} - X_2}{2X_{mix} + (X_2/y_2)(\sigma_2+1)} = 0 \\ \\ (1-\eta_2)\dfrac{X_{mix}/y - X_1/y_1}{2X_{mix} + (X_1/y_1)(\sigma_1+1)} + \\ \quad +\eta_2 \dfrac{X_{mix}/y - X_2/y_2}{2X_{mix} + (X_2/y_2)(\sigma_2+1)} = 0 \end{cases}, \tag{9}$$

where (omitting the subscripts for notational ease)

$$X = \frac{\sigma Y}{\sigma + 1},\ y = \sigma - 2. \tag{10}$$

Plane-stratified mixtures [40] where each layer is very thin (with typical thicknesses of a few nm) compared to the relevant optical (and acoustic) wavelengths, as an alternative to co-sputtered glassy mixtures (see Figure 7). Such composites will be henceforth referred to as nanolaminates, or nanolayered materials. Their macroscopic properties are amenable to elementary modeling, which makes them easily engineerable. Nanolayered materials attain limit-

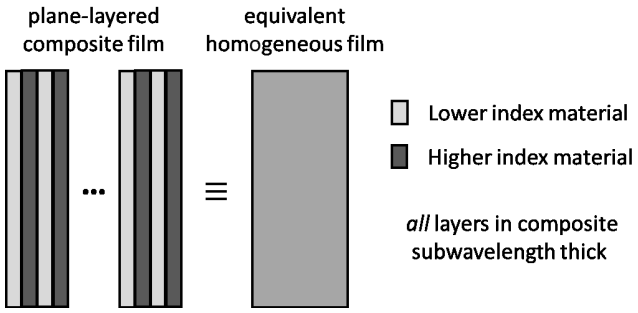

Fig. 7. Sketch of a binary nanolayered material.

ing values for both their effective refractive index and Young's modulus. Their effective dielectric constant ε_{mix} for normal plane-wave incidence is given by Drude's formula [41],

$$\varepsilon_{mix} = (1 - \eta_2)\varepsilon_1 + \eta_2 \varepsilon_2. \tag{11}$$

Their elastic Young modulus for normal and transverse stresses attain the Reuss and Voigt bounds [42], [43], respectively, viz.

$$Y_{\perp} = \frac{Y_1 Y_2}{\eta_2 Y_1 + (1 - \eta_2) Y_2}, \tag{12}$$

and

$$Y_{||} = \eta_2 Y_2 + (1 - \eta_2) Y_1, \tag{13}$$

and their effective mechanical loss angle can be readily computed using eqs. (2), (3).
In Figure 8 co-sputtered and nanolayered Titania/Silica mixtures are compared in terms of refractive index and specific loss angles, using EMT. Nanolayered composites turn out to be optically denser compared to cosputtered mixtures with the same composition, and also less noisy, for the same refractive index.
Another appealing feature of nanolayered composites is their ability to hinder crystallization upon thermal annealing observed in materials like HfO_2, TiO_2, and ZrO_2 [44], [45]. Post deposition thermal annealing improves optical and mechanical film quality, by releasing internal stresses [46], but subsequent crystallization makes scattering and mechanical losses blow up [44]. Nanolayered composite films with the same effective parameters (refraction index, Young modulus, loss angle, depending only on the constituents fractions, represented by the single parameter η_2) can be designed using layers of different thicknesses. Silica/Titania laminates with thinner layers are known to tolerate higher annealing temperatures before crystallization sets in [47]. Nanolayered HfO_2/Al_2O_3 composites behave similarly [48].

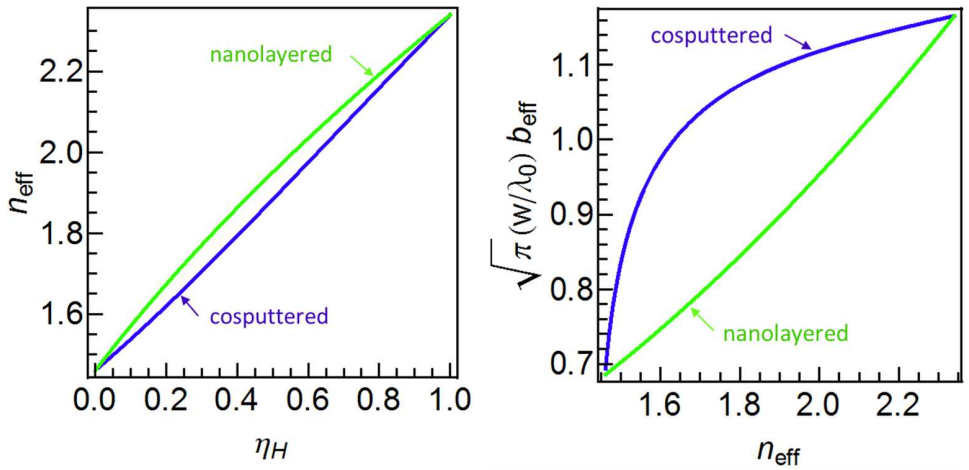

Fig. 8. Cosputtered vs nanolayered Silica-Titania mixtures. Left: effective refraction index vs volume fraction η_H of Titania. Right: effective specific loss angles, eq. (3) vs effective refraction index.

This suggests that glass-former nanolayers may act as buffers, preventing the growth of crystallites formed during deposition in the other material.
Prototypes of nanolayered Silica/Titania composite films were designed, produced and tested in a cooperation between our group at the University of Sannio, and the group led by prof. S. Chao, at the National Tsing Hua University of Taiwan, ROC, in the frame of the LIGO-Virgo Collaboration. The NTHU Kaufman-type ion beam sputterer facility is shown in figure 9 . All prototypes had the same effective refractive index $n_{eff} = 2.065$, but different layer thicknesses, in a range from a few nm to a few tens nm, and a correspondingly different number of nanolayers, such as to make them all QWL thick at the reference wavelength of 1064 nm.

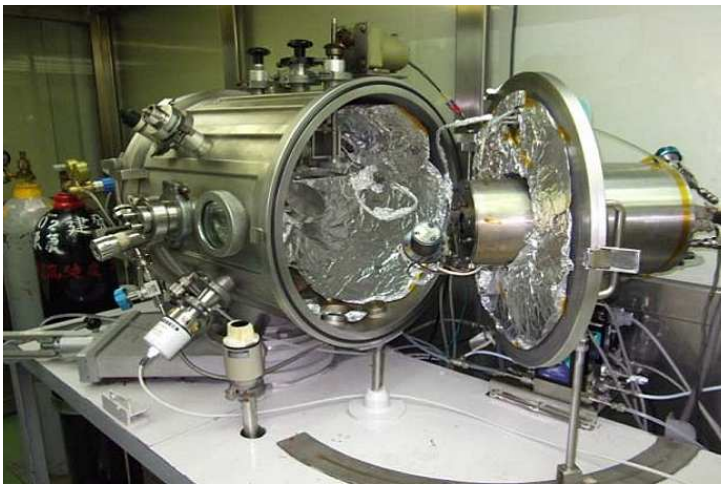

Fig. 9. The NTHU deposition facility used to produce the nanolayer prototypes is a Kaufman-type ion beam sputterer is located in a Class-100 clean compartment, within Class-10000 clean room (courtesy S. Chao).

Figure 10, shows the X-ray diffraction spectra of several nanolayered prototypes made at

NTHU after annealing at 300*C* for 24*h*. As the number of layers increases (and the layers be-

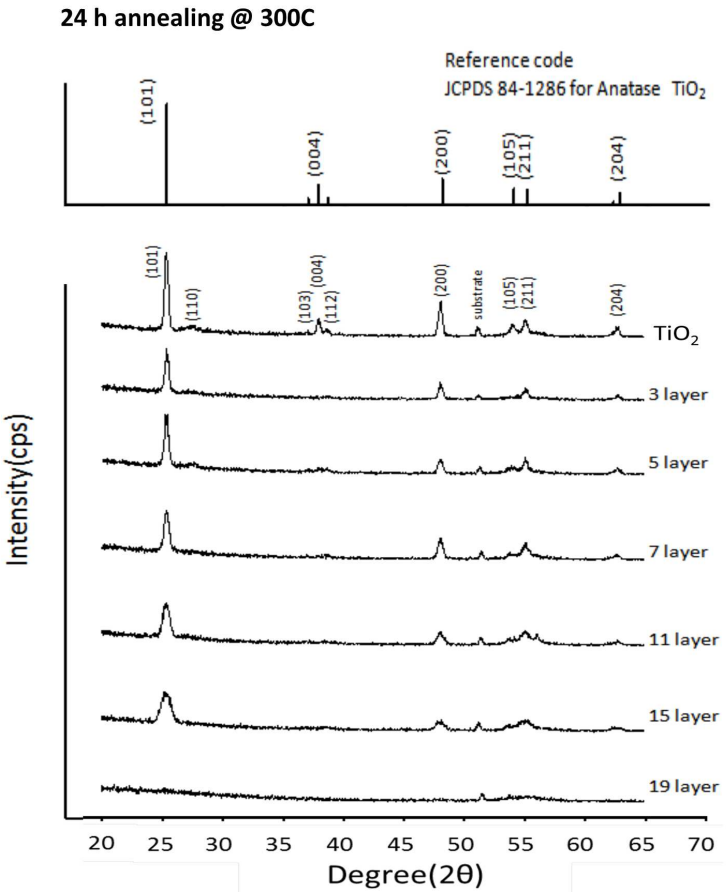

Fig. 10. X-ray diffraction spectra of different Titania/Silica nm-layered films, after 24h annealing @ 300C. All films are designed to have the same refractive index and optical thickness, but differ in the total number and thickness of the individual layers. [49].

come correspondingly thinner), the X-ray diffraction peaks signaling crystallization gradually disappear [49]. Correspondingly, the TEM and electron-diffraction images of the 19-layers prototype, shown in figure 11, are basically the same before and after annealing, and show no visible hint of crystallization.
Preliminary loss angle measurements on annealed nanolayered Titania/Silica films appear encouraging [50].

It is worth noting here that the technology of nm-layered optical coatings has progressed significantly during the last decade, in connection with frontier applications ranging from extreme-UV litography to X and soft-gamma ray optics [51], [52].
Here technological challenges may be milder, since stringent requirements on the *individual* layers thickness accuracies are *not* imposed.

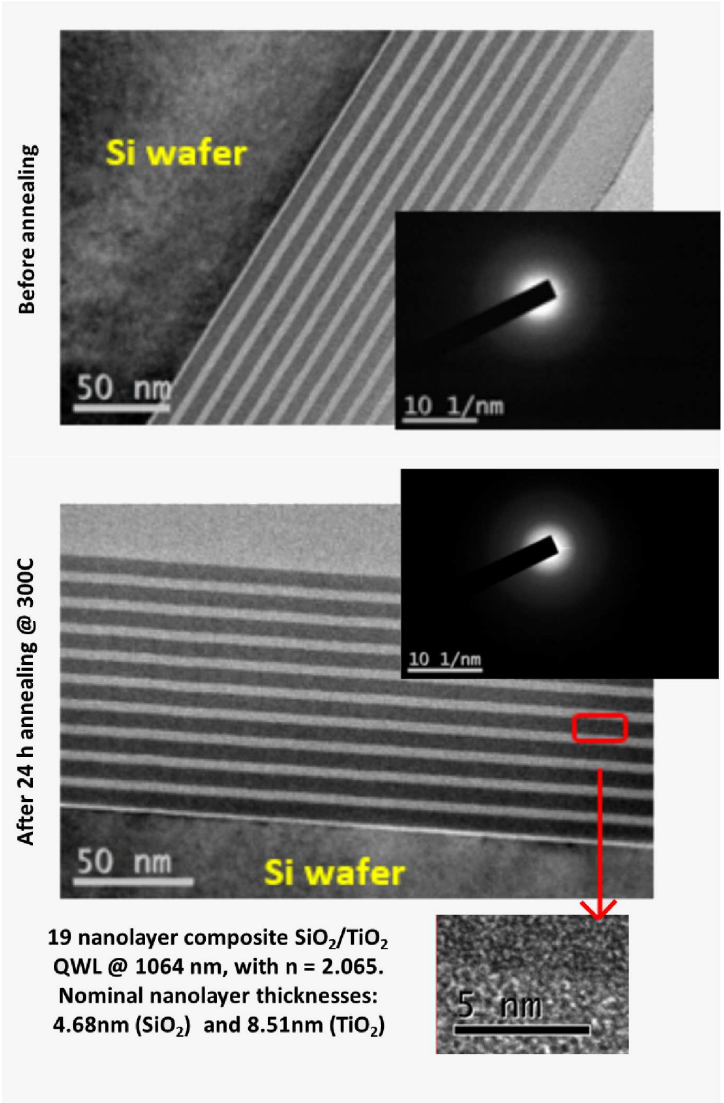

Fig. 11. TEM image and electron diffraction pattern of 19 nanolayers QWL prototype, as deposited (top), and after 24h annealing at $T = 300C$ (bottom).

5. More Coating Noise Reduction Strategies

In this Section I present a compact overview of other coating noise reduction strategies proposed so far.

5.1. Low Temperatures

Lowering the temperature does not reduce coating Brownian noise as much as one would expect from eq. (1). Indeed, most coating materials, including Silica and Tantala (plain as well as TiO_2-doped) exhibit a mechanical-loss peak at some temperature in the $10 - 100K$ range (see Figure 12 and [53]), whose height and width depend on the material composition, and the

post-deposition annealing schedule [54]. Hafnia (HfO_2) and Titania (TiO_2) are notable exceptions [55], [56]. As already mentioned, both Hafnia and Titania tend to crystallize during post deposition annealing, but this difficulty can be circumvented by doping (co-sputtering) these materials with good glass formers, like Silica [57], is effective in stabilizing several materials against thermal-annealing induced crystallization, including Titania [58], Hafnia and Zirconia [45].
Remarkably, Silica doping does *not* affect the nice low-temperature properties of Hafnia [59]. Cryogenic loss measurements on Silica doped Titania and nanolayered Silica/Titania and/or Silica/Hafnia composites are underway [60].

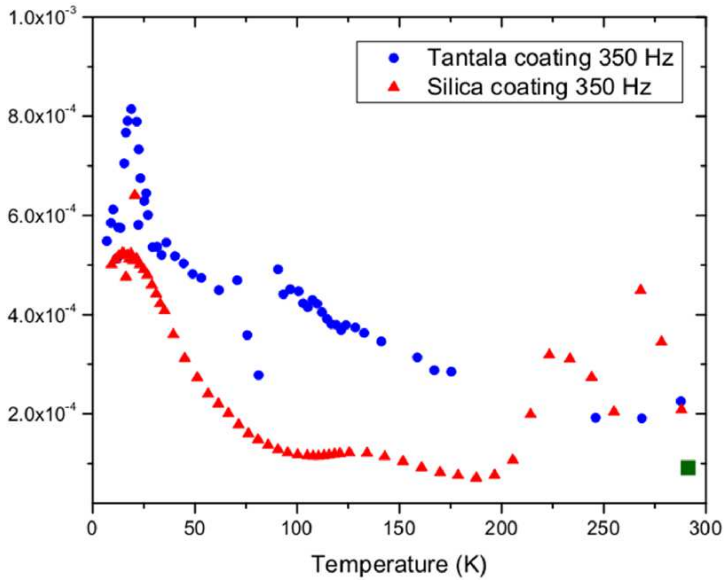

Fig. 12. Mechanical losses vs temperature, from [53]. Losses increase upon reducing temperature, peaking at a certain temperature.

5.2. *Wide Beams*

Wide beams are effective in reducing coating noise by averaging out thermal fuctuations of the mirror surface over a larger illuminated area. Different families of "wide beams" have been proposed so far, including "mesa" [61], hyperbolic [62] and Bessel beams [63]. See [64] for a broad discussion.
Gauss Laguerre modes, in particular, received considerable attention, since they may fit standard spherical-mirror cavities [65], although imposing much tighter mode-matching and astigmatism requirements [66].

5.3. *Radical Alternatives*

A number of radical alternatives to present-day mirrors based on amorphous glassy oxide dielectric coatings, have also been proposed. Among these: replacing the mirrors with anti-resonant cavities obtained by leaving only a few coating layers on the front face of transparent test masses, and placing the remaining ones on the back face (Khalili etalons [67]); adopting

non-diffractive, coating-free mirrors, based on total internal reflection and Brewster-angle coupling [68]; using diffractive (grating-based) monolithic (e.g., Silicon or Sapphire) mirrors [69]; taking advantage of the extreme low losses of epitaxially grown single-crystalline coatings, e.g., *GaAs/AlGaAs* [70] or *GaP/AlGaP* [71]. All these ideas hold significant potential and are being actively explored, but each of them faces specific technological and/or conceptual problems that hinder, at present, their immediate full-scale applicability to GW detectors.

6. Conclusions

Coating design optimization for thermal (Brownian) noise minimization in the test-mass mirrors of interferometric detectors of gravitational waves has been reviewed, with emphasis on geometric (thickness) and materials' (mixing) optimization.
Among all test-mass Brownian noise reduction techniques proposed so far, coating thickness optimization is undoubtedly the simplest, best understood, technologically less demanding and cheapest option, capable of reducing the coating noise power spectral density level by a factor ~ 0.8, and correspondingly boosting the instrument's visibility distance by a round $\sim 30\%$.
Coating materials optimization has already led significant results, based on extensive trial and error testing of different amorphous glassy oxide mixtures, and there is still room for significant improvements, in the perspective of third generation (cryogenic) detectors. Nanolayered composites are an interesting option, but need to be investigated further to assess their potential, and technological challenges.

Acknowledgments

The work described in this paper has been done within the LIGO-Virgo Collaboration (LVC), in collaboration with Akira E. Villar, Eric D. Black, Kenneth G. Libbrecht (Caltech); Christophe Michel, Nazario Morgado, Laurent Pinard (LMA), Shiuh Chao, Ling-Chi Kuo, Huang-Wei Pan, Julie Wang (NTHU), Giuseppe Castaldi, Riccardo DeSalvo, Vincenzo Galdi, Vincenzo Pierro, Innocenzo M. Pinto, Ilaria Taurasi (University of Sannio); and has been sponsored in part by the Italian National Institute for Nuclear Physica (INFN), under the AdCOAT, COAT, and MIDI-BRUT grants; the US National Science Foudation, under the Cooperative Agreement PHY-0757058); and the National Science Council of Taiwan, ROC, under the NSC-100-2221-E-007-099 project. Special thanks are due to Gregory M. Harry, Jean-Marie Mackowsky, Iain Martin, Ronny Nawrodt and Steve Penn for kind encouragement and stimulating discussions.